

**UNCLASSIFIED**

---

---

**AD 260 534**

*Reproduced  
by the*

**ARMED SERVICES TECHNICAL INFORMATION AGENCY  
ARLINGTON HALL STATION  
ARLINGTON 12, VIRGINIA**



---

---

**UNCLASSIFIED**

**NOTICE:** When government or other drawings, specifications or other data are used for any purpose other than in connection with a definitely related government procurement operation, the U. S. Government thereby incurs no responsibility, nor any obligation whatsoever; and the fact that the Government may have formulated, furnished, or in any way supplied the said drawings, specifications, or other data is not to be regarded by implication or otherwise as in any manner licensing the holder or any other person or corporation, or conveying any rights or permission to manufacture, use or sell any patented invention that may in any way be related thereto.

CATALOGED BY ASTIA  
AS AD No. \_\_\_\_\_

260534

Technical Report No. 1

Project No. A-519

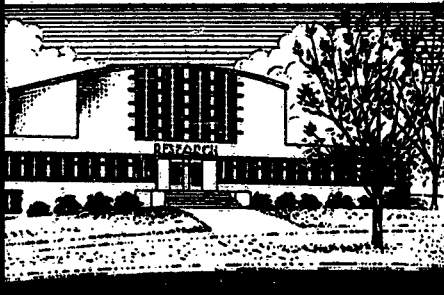
Acoustic Modulation of The Conductivity  
of Salt Solutions

By

W. K. Rivers, Jr., D. F. Eagle, J. R. Walsh, Jr.  
and D. J. Bryant

28 June 1961

U. S. Navy Department  
Office of Naval Research  
Contract Nonr-991(08)  
NR 371-330



Engineering Experiment Station  
Georgia Institute of Technology  
Atlanta, Georgia

61-4-1  
XEROX

ENGINEERING EXPERIMENT STATION  
of the Georgia Institute of Technology  
Atlanta, Georgia

TECHNICAL REPORT NO. 1

PROJECT NO. A-519

ACOUSTIC MODULATION OF THE CONDUCTIVITY  
OF SALT SOLUTIONS

By

W. K. RIVERS, JR., D. F. EAGLE, J. R. WALSH, JR.  
and D. J. BRYANT

28 JUNE 1961

U. S. NAVY DEPARTMENT  
OFFICE OF NAVAL RESEARCH  
CONTRACT Nonr-991(08)  
NR 371-330

ABSTRACT

The fractional change of the conductivity of aqueous sodium chloride solutions produced by an acoustic wave has been measured and found to be  $0.7 \times 10^{-10}$  per dyne/cm<sup>2</sup> pressure change at room temperature over a concentration range of 0.3 to 3.0 molal. The measurements are consistent with predictions based on theory and static data and with previous measurements of the change in the low-frequency bulk conductivity of salt water produced by an acoustic wave. The measurements were made by reflecting electromagnetic and acoustic waves from the salt water surface in a coaxial test cell at a radio frequency of 146 mc and acoustic frequencies in the range of 15 to 30 kc. The equipment used is capable of measuring an amplitude modulation index lower than 160 db below 100 per cent for one cycle per second of bandwidth.

TABLE OF CONTENTS

	Page
I. INTRODUCTION	1
II. ACOUSTIC-RADIO INTERACTION	3
A. Modulation of an Electromagnetic Wave by an Acoustic Wave	
B. Modulation Due to Surface Motion	
C. Predicted Perturbations	
D. Instrumentation	
E. Results of Measurements	
III. SUMMARY	23
IV. ACKNOWLEDGMENTS	24
V. APPENDIX	25
A. Radio-Frequency Equipment	
B. Acoustic Equipment	
C. Measurement Procedure	

This report contains 40 pages.

LIST OF FIGURES

	Page
1. Modulation of an Electromagnetic Wave by a Sound Wave	4
2. Amplitude Modulation per Fractional Change of Conductivity of Salt Water	8
3. Equipment for Measurement of Acoustic-Radio Interaction	18
4. Experimentally Determined Amplitude Modulation Index per Unit Pressure for Aqueous Sodium Chloride Solutions at 27° C	20
5. Amplitude Detector	27
6. Spectrum of Amplitude Modulated Carrier	29
7. Minimum Detectable Modulation Index of Amplitude Detectors for a Bandwidth of One Cycle per Second	33
8. Acoustic Probe Construction	36
9. Coaxial Test Cell	37

LIST OF TABLES

	Page
I. PREDICTED FRACTIONAL CHANGE OF CONDUCTIVITY	13
II. PREDICTED FRACTIONAL CHANGE OF DIELECTRIC CONSTANT	17
III. COMPARISON OF EXPERIMENTALLY DETERMINED AND PREDICTED VALUES OF $g$	21
IV. OPERATING PARAMETERS OF RADIO FREQUENCY GENERATOR OUTPUT AMPLIFIER	26
V. COMPARISON OF SIGNAL AND NOISE POWERS BEFORE AND AFTER DETECTION	30
VI. SUMMARY OF PROBE CALIBRATION DATA	34

GLOSSARY

<u>Symbol</u>	<u>Meaning</u>
a	Used as a subscript to denote an acoustic quantity
c	Velocity of propagation of radio waves in vacuum
$c_a$	Velocity of propagation of acoustic waves in water
$C_p$	Specific heat at constant pressure
E	Voltage; electric field
$f = d\epsilon_r/\epsilon_r$	Fractional change of dielectric constant per dyne/cm <sup>2</sup> pressure change
$g = d\sigma/\sigma$	Fractional change of conductivity per dyne/cm <sup>2</sup> pressure change
$g_m$	Diode conductance
G	Mixer conversion gain
i	Imaginary unit; numerical subscript
Im(m)	Imaginary part of modulation index, denotes phase modulation
k	Boltzmann's constant
$K = c_a/c$	Ratio of acoustic and radio velocities of propagation in their respective media
$K_a$	Acoustic propagation constant
$K_2$	Radio propagation constant in water
m	Modulation index
n	Optical index of refraction
N	Number per unit volume
$N_c$	Noise ratio of crystal diode
$N_d$	Noise ratio of thermionic diode

GLOSSARY (Continued)

<u>Symbol</u>	<u>Meaning</u>
$P$	Pressure
$P_a$	Peak acoustic pressure
$P$	Power
$R_{nf}$	Flicker noise resistance
$Re(m)$	Real part of $m$ , denotes amplitude modulation
$t$	Time
$T$	Temperature
$V$	Specific volume
$Z_1$	Radio wave impedance in vacuum
$Z_2$	Radio wave impedance in water
$\beta$	Volume coefficient of expansion
$\gamma_c$	Noise constant for crystal diode
$\gamma_d$	Noise constant for thermionic diode
$\delta$	Peak displacement of surface
$\Delta$	Used to denote a small change in a quantity
$\epsilon$	Complex relative permittivity of salt solution
$\epsilon_r$	Dielectric constant or real part of $\epsilon$
$\lambda$	Radio wavelength in vacuum
$\lambda_a$	Acoustic wavelength in water
$\mu$	Ion mobility; micro-
$\mu_o$	Molecular electric dipole moment

GLOSSARY (Continued)

<u>Symbol</u>	<u>Meaning</u>
$\nu$	Radio frequency
$\nu_a$	Acoustic frequency
$\omega$	Radio angular frequency
$\omega_a$	Acoustic angular frequency
$\rho$	Density
$\sigma$	Conductivity in esu, related to conductivity in mks units, $\sigma_{\text{mks}}$ , by $\sigma = \frac{\sigma_{\text{mks}}}{4\pi\epsilon_0}$

## I. INTRODUCTION

The interaction of acoustic and electromagnetic waves takes place in a dielectric medium. An acoustic wave in this material causes local variations in density and temperature, which produce small changes in the electromagnetic parameters of the material: the dielectric constant and the conductivity. It is with the perturbations of these properties of aqueous salt solutions that the work described in this report is concerned.

The alteration of the conductivity of salt water by acoustic waves has been studied previously by Fox, Herzfeld, and Rock.<sup>1</sup> They measured the change in conductivity of a salt solution at a radio frequency of 4 kc caused by acoustic waves in the frequency range 0.5 to 2 mc. They predicted that the conductivity would be perturbed by about a part in  $10^{10}$  per dyne/cm<sup>2</sup> of acoustic pressure, and approximate confirmation of this was observed experimentally.

The present experiment is directed toward an accurate measurement of the acoustic perturbation of both the dielectric constant and the conductivity of aqueous salt solutions. The geometry is one in which the electromagnetic waves and acoustic waves are normally incident on an air, salt water interface; the waves are confined to a coaxial pipe in order that the pressure and modulation may be accurately determined. Both waves are reflected at the surface, because a large impedance discontinuity is seen by each. Because the dielectric properties are modulated periodically by the acoustic standing wave, the reflected electromagnetic wave includes sidebands representing modulation at the acoustic

---

<sup>1</sup>F. E. Fox, K. F. Herzfeld and G. D. Rock, "The Effect of Ultrasonic Waves on the Conductivity of Salt Solutions," Physical Review 70, 329 (1946).

frequency. The modulation is of both the phase and the amplitude of the reflected carrier. Since surface motion also modulates the phase of the reflected signal, observation of the amplitude modulation only is necessary to give a quantitative measurement of the desired perturbation.

The amount of modulation produced is a function of the relative wavelengths in the water; if the electromagnetic losses in the water were low, the reflection would strongly resemble the Bragg reflection exhibited by X-rays from the planes of a crystal. However, in a strong electrolyte, most of the interaction takes place near the surface, and the frequency dependence of the interaction is weak.

Measurements have been made at a radio frequency of 146 mc and acoustic frequencies in the range 15 kc to 30 kc on sodium chloride solutions of concentration 0.3, 0.6, 1.5 and 3.0 molal and on Subow's<sup>2</sup> sea water mixture. At these frequencies, the amplitude modulation is almost entirely due to conductivity perturbation. Further measurements are planned at a radio frequency of about 1000 mc in order to provide an accurate estimate of the dielectric constant perturbation.

---

<sup>2</sup>American Institute of Physics Handbook, McGraw-Hill Book Company, New York (1957), p. 3-70.

II. ACOUSTIC-RADIO INTERACTION

A. Modulation of an Electromagnetic Wave by an Acoustic Wave

The theory of reflection of electromagnetic waves from sound waves has been explored by Schmitt and others.<sup>3,4,5,6</sup> Their results, which followed from considering unbounded plane waves above and below the interface, as in Figure 1, are applicable to the coaxial geometry of the present experiment. This follows because the impedances definable in the plane wave case are exactly the same as for the fundamental mode in coaxial tubing, and no nonlinearities in the field magnitudes are known to exist. Schmitt's results will be used directly, and no attempt will be made here to develop the theory.

An easily measured quantity is the modulation index,  $m$ , of the reflected electromagnetic wave, which is defined by:

$$E = E_0(1 + m \cos \omega_a t)$$

In reference 3, Schmitt derived an approximate expression for  $m$  due to sound pressure modulation of the complex relative permittivity,  $\epsilon$ , of the water. It is

---

<sup>3</sup>H. J. Schmitt, "Reflection of Electromagnetic Waves from Sound Waves," Cruft Laboratory, Harvard University, Technical Report No. 310a, 5 January 1960.

<sup>4</sup>H. J. Schmitt and D. Sengupta, "On the Reflection of Electromagnetic Waves from a Medium Excited by Acoustic Waves," Journal of Applied Physics 31, 439 (1960).

<sup>5</sup>H. J. Schmitt and T. T. Wu, "Electromagnetic Reflection from Sound Waves," Cruft Laboratory, Harvard University, Technical Report No. 317, 1 March 1960.

<sup>6</sup>H. J. Schmitt and T. T. Wu, "Electromagnetic Reflection from Sound Waves," Journal of the Acoustical Society of America 32, 1660 (1960).

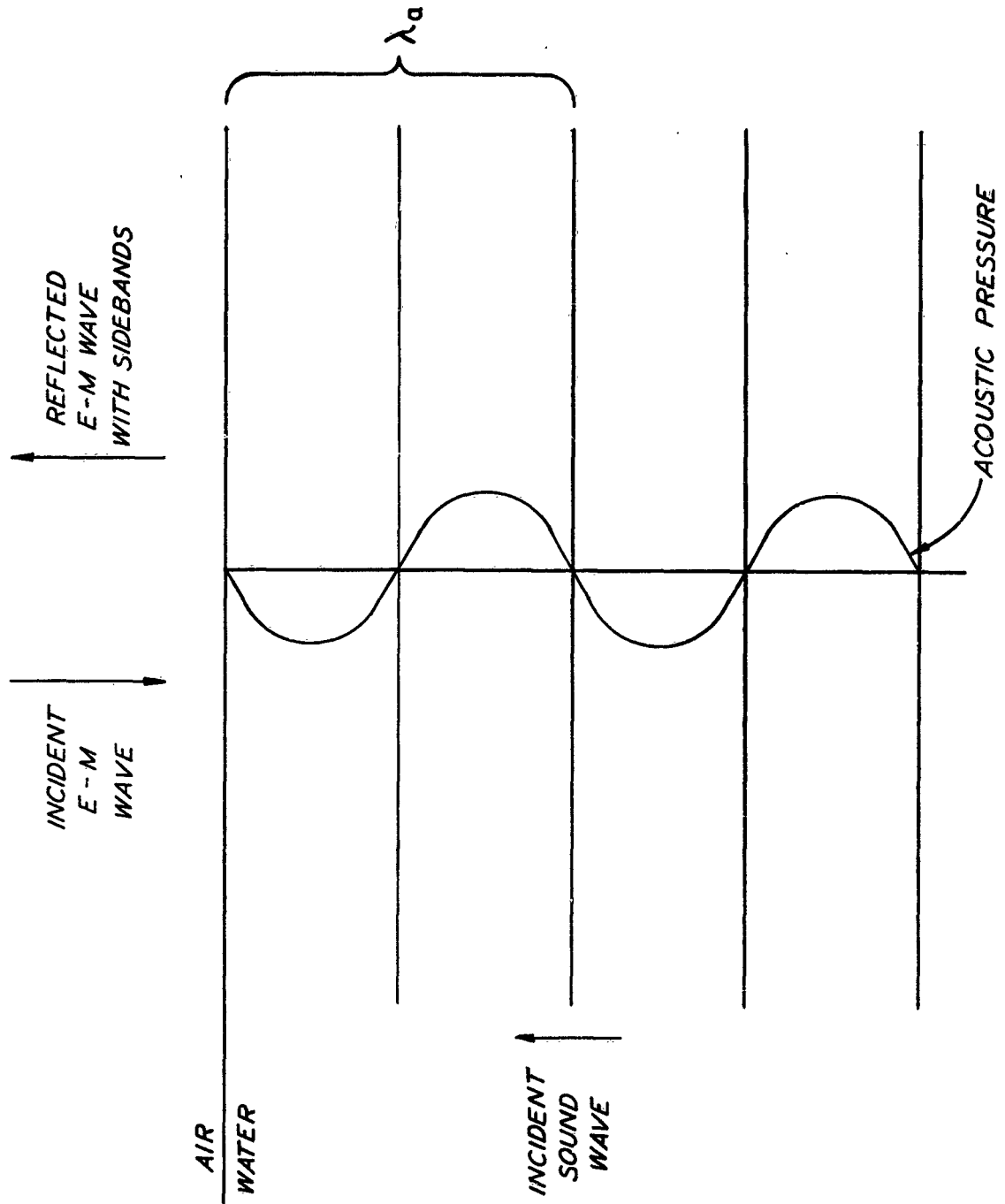


Figure 1. Modulation of an Electromagnetic Wave by a Sound Wave.

$$m = \frac{2i \frac{Z_2}{Z_1} \frac{K_a}{K_2} \frac{\Delta\epsilon}{\epsilon}}{\left[ \left( \frac{Z_2}{Z_1} \right)^2 + 1 \right] \left[ 4 - \left( \frac{K_a}{K_2} \right)^2 \right]}, \quad (1)$$

in which  $Z_1$  is the wave impedance in air,

$Z_2$  is the wave impedance in water,

$K_a = \frac{2\pi}{\lambda_a}$ ;  $\lambda_a$  is the acoustic wavelength,

$K_2 = \frac{\omega}{c} \sqrt{\epsilon}$  is the electromagnetic propagation constant in the water.

$\epsilon = \epsilon_r - i2\sigma/\nu$ .  $\epsilon_r$  is the dielectric constant of the water, and  $\sigma$  is its conductivity in electrostatic units.  $\sigma$  is related to the conductivity in mks units,  $\sigma_{mks}$ , by  $\sigma = \sigma_{mks}/(4\pi\epsilon_0)$ .

$\Delta\epsilon/\epsilon$  is the peak fractional change in complex permittivity at a distance  $\lambda_a/4$  below the surface of the water where the pressure is a maximum.

Equation 1 may be simplified by noting that  $|(Z_2/Z_1)^2| \ll 1$ , and it may be written in the form

$$m = \frac{2i \frac{\lambda_a}{\lambda} \frac{\Delta\epsilon}{\epsilon}}{1 - 4 \left[ \frac{\lambda_a}{\lambda} \right]^2 (\epsilon_r - i2\sigma/\nu)} \quad (2)$$

in which  $\nu$  is the radio frequency.

Let  $f = d\epsilon_r/\epsilon_r$  and  $g = d\sigma/\sigma$  be the fractional changes of the dielectric constant and conductivity, respectively, per dyne/cm<sup>2</sup> pressure change. Then the fractional change in permittivity can be written

$$\frac{\Delta\epsilon}{\epsilon} = p_a \frac{f\epsilon_r - ig2\sigma/v}{\epsilon_r - i2\sigma/v}, \quad (3)$$

where  $p_a$  is the peak acoustic pressure at a depth of  $\lambda_a/4$ . If this is substituted into Equation 2 and the real part of  $m$  (corresponding to amplitude modulation of the reflected wave) is found, one obtains:

$$\text{Re}(m) = \frac{4K\sigma v_a^2 g p_a}{\epsilon_r^2 v^2 + 4\sigma^2} \left\{ \frac{\epsilon_r v_a^2 + 16K^2 \sigma^2 - 4K^2 v^2 \epsilon_r + \frac{f}{g} (8K^2 v^2 \epsilon_r^2 - \epsilon_r v_a^2)}{v_a^4 - 8K^2 v^2 v_a^2 \epsilon_r + 16K^4 (\epsilon_r^2 v^4 + 4\sigma^2 v^2)} \right\}, \quad (4)$$

in which  $v$  is the radio frequency,

$v_a$  is the acoustic frequency,

$K = c_a/c$ , where  $c_a$  is the speed of sound in the water,  $c$  the speed of light in air.

Although not useful here, the imaginary part of  $m$  obtained from Equation 2 is given for completeness.

$$\text{Im}(m) = \frac{2Kv v_a g p_a}{\epsilon_r^2 v^2 + 4\sigma^2} \left\{ \frac{4\sigma^2 v_a^2 - 32K^2 \sigma^2 \epsilon_r v^2 + \frac{f}{g} (\epsilon_r^2 v^2 v_a^2 + 16K^2 v^2 \sigma^2 \epsilon_r - 4K^2 v^4 \epsilon_r^3)}{v_a^4 - 8K^2 v^2 v_a^2 \epsilon_r + 16K^4 (\epsilon_r^2 v^4 + 4\sigma^2 v^2)} \right\}.$$

It is of interest that Equation 4 can be made independent of the dielectric constant variation by requiring that

$$8K^2 v^2 \epsilon_r^2 - \epsilon_r v_a^2 = 0 \quad (5)$$

For this condition, the frequencies are related by

$$v_a = 2\sqrt{2\epsilon_r}Kv$$

In Figure 2, the real part of  $m$  divided by  $gp_a$  is plotted against the radio frequency,  $\nu$ , for several assumed values of the ratio  $f/g$ . These curves were obtained from Equation 4 for the following values of the constants:

$$\begin{aligned}v_a &= 17.5 \text{ kc,} \\ \sigma &= 4.5 \times 10^{10} \text{ esu,} \\ \epsilon_r &= 69, \\ c_a &= 1520 \text{ m/sec.}\end{aligned}$$

These values of  $\sigma$  and  $\epsilon_r$  are representative of 0.6-molal salt solution at 20° C over the frequency range  $0 \leq \nu \leq 1000 \text{ mc.}^7$

Examination of the curves in Figure 2 shows two features of particular interest:

(1) The modulation produced by the acoustic wave is independent of the assumed ratio  $f/g$  at a radio frequency of 146 mc and is caused solely by the variation in conductivity;

(2) Once the conductivity perturbation constant,  $g$ , is known, the greatest resolution for a determination of the dielectric constant coefficient,  $f$ , will be obtained at a radio frequency of about 1000 mc.

If the conductivity perturbation is of the order of  $10^{-10}$  per dyne/cm<sup>2</sup> and the acoustic pressure is  $10^5$  dyne/cm<sup>2</sup>, then one might expect to measure an amplitude modulation index of about  $2 \times 10^{-7}$  at radio and acoustic frequencies of 146 mc and 17.5 kc, respectively.

---

<sup>7</sup>J. A. Saxton and J. A. Lane, "Electrical Properties of Sea Water," Wireless Engineer 29, 269 (1952).

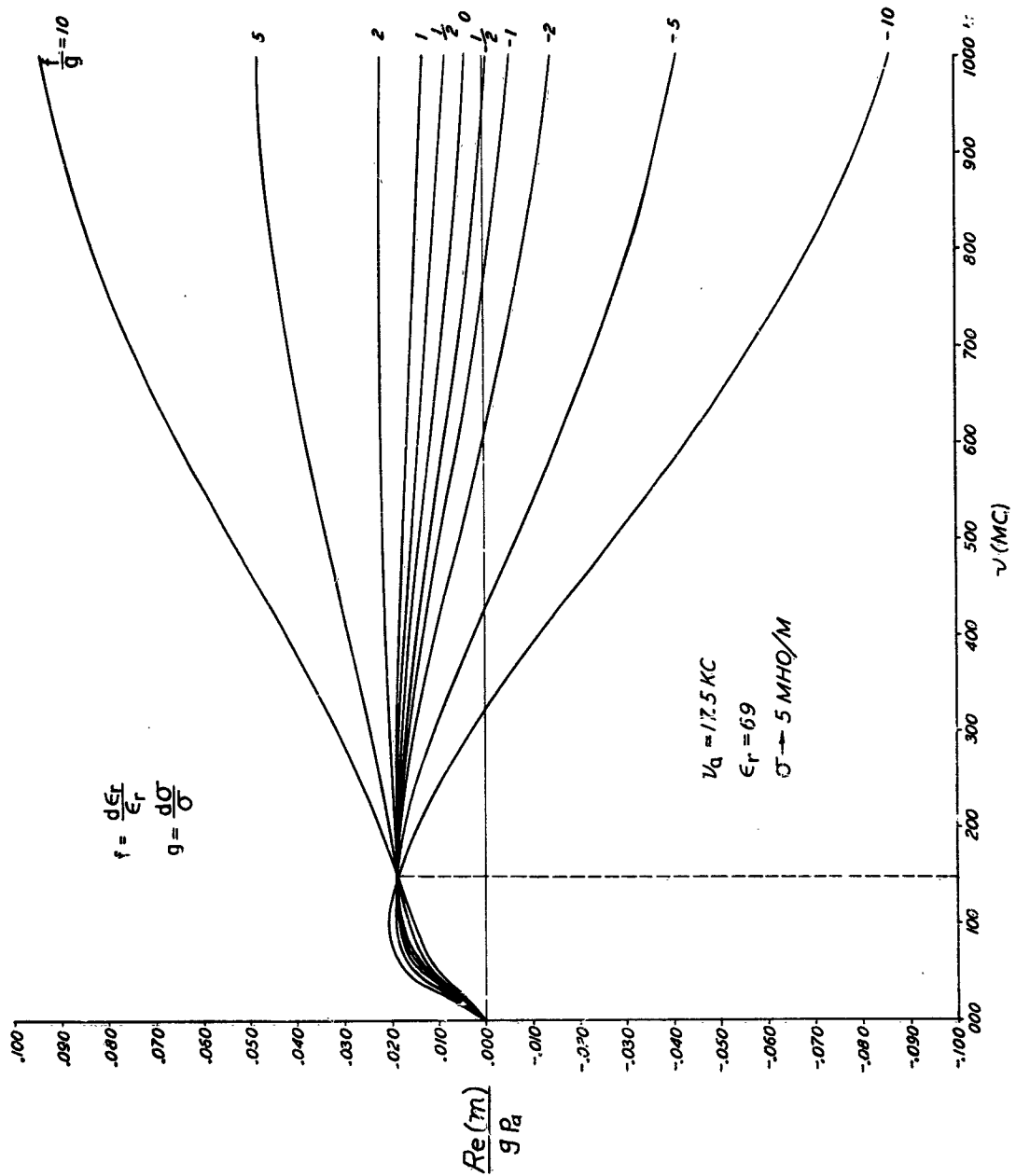


Figure 2. Amplitude Modulation per Fractional Change of Conductivity of Salt Water.

B. Modulation Due to Surface Motion

The acoustic standing wave in the water results from the requirement that a pressure node exist at the surface. At this point, the particle displacement,  $\delta$ , is a maximum;  $\delta$  is related to the peak pressure,  $p_a$ , at a position  $\lambda_a/4$  below the surface by<sup>8</sup>

$$\delta = \frac{p_a}{\omega_a \rho c_a}$$

This surface displacement produces a modulation of the phase of the r-f signal reflected from the water; the corresponding modulation index,  $m_s$ , is given by

$$m_s = \frac{2ip_a}{\rho c c_a} \cdot \frac{v}{v_a}$$

For acoustic and radio frequencies of 17.5 kc and 146 mc, respectively,  $m_s$  is about  $1(3.6 \times 10^{-12})$  per dyne/cm<sup>2</sup> peak acoustic pressure. This is of the same order as the modulation produced by the conductivity perturbation. If the effects of the conductivity and dielectric constant perturbations are to be separated from the effect of surface movement, then the detection must be made in such a manner that the relative phase of the carrier and sidebands is not disturbed by the r-f components between the reflecting surface and the detector, and use must be made of a detector which is insensitive to phase modulation. In this experiment, particular attention was paid to these considerations.

---

<sup>8</sup>P. M. Morse, Vibration and Sound, McGraw-Hill Book Company, New York (1948).

C. Predicted Perturbations

1. Temperature and Density Changes

A theoretical prediction of the perturbation of the dielectric properties of salt water caused by the presence of a sound wave was made. The pressure fluctuation in the sound wave affects the medium by producing local variations in temperature and density. These two effects are directly responsible for perturbing the conductivity and the dielectric constant of the salt water. In the following treatment, the conductivity and dielectric constant are assumed to be functions of the two independent variables, temperature and density.

If an adiabatic process is assumed, the temperature change is given by:<sup>9</sup>

$$\begin{aligned} \Delta T &= \frac{T}{C_p V} \left( \frac{\partial V}{\partial T} \right)_p \Delta p \\ &= \frac{T}{C_p} \beta \Delta p \quad , \end{aligned}$$

where T is the Kelvin temperature,

$C_p$  is the specific heat at constant pressure,

$\beta = \frac{1}{V} \left( \frac{\partial V}{\partial T} \right)_p$  is the volume coefficient of expansion,

$\Delta p$  is the pressure change due to the sound wave.

For  $T = 25^\circ \text{C} = 298.2^\circ \text{K}$ , at which  $C_p = .932 \text{ cal/gm/deg} = 3.901 \times 10^7 \text{ erg/gm/deg}$ , and  $\beta = 2.86 \times 10^{-4}$  per degree,<sup>10</sup>

$$\Delta T = 2.19 \times 10^{-9} \text{ }^\circ\text{C per dyne/cm}^2 \text{ pressure change.}$$

<sup>9</sup>J. K. Roberts and A. R. Miller, Heat and Thermodynamics, Interscience Publishers, New York (1960), p. 586.

<sup>10</sup>American Institute of Physics Handbook, McGraw-Hill Book Company, New York (1957), p. 2-118.

From the acoustic relation for the velocity of sound in a liquid,

$$c_a^2 = \left( \frac{\partial p}{\partial \rho} \right)_s ,$$

the density change is obtained as

$$\Delta \rho = \frac{\Delta p}{c_a^2} ,$$

where  $c_a$  is the velocity of sound, and  $\Delta p$  has the same meaning as before. For sea water,  $c_a \approx 1520$  m/sec, and

$$\Delta \rho = 4.3 \times 10^{-11} \text{ gm/cm}^3 \text{ per dyne/cm}^2 \text{ pressure change.}$$

## 2. Conductivity

From the data of Saxton and Lane, empirical expressions of the form

$$\sigma(T) = A + BT \tag{6}$$

can be derived for conductivity as a function of temperature over the range 0 to 40° C. In this expression,  $\sigma$  is the conductivity in esu,  $T$  is the temperature in degrees centigrade, and  $A$  and  $B$  are constants depending on the concentration. Values of these constants for four different concentrations of aqueous sodium chloride solutions are listed below:

<u>Molality</u>	<u>A x 10<sup>-11</sup></u>	<u>B x 10<sup>-11</sup></u>
0.3	0.148	0.00507
0.6	0.265	0.00938
1.5	0.60	0.0188
3.0	0.98	0.0319

From the definition of  $g$  and Equation 6, it follows that

$$g(T) = \left( \frac{\Delta\sigma}{\sigma} \right)_p = \frac{B\Delta T}{A + BT}$$

To relate conductivity to density, assume that for a particular ion species the contribution to the conductivity is proportional to the charge carried by an ion, to the ion mobility, and to the number of ions present. Thus

$$\sigma_i = q_i \mu_i N_i$$

where, for the  $i^{\text{th}}$  type of ion,  $\sigma_i$  is the conductivity,

$\mu_i$  is the mobility,

$q_i$  is the valence charge,

$N_i$  is the number per cubic centimeter.

The total conductivity,  $\sigma$ , is the sum of the partial conductivities,  $\sigma_i$ .

Therefore,

$$\sigma = \sum_i \sigma_i = \sum_i q_i \mu_i N_i$$

Assume further that  $q_i$  and  $\mu_i$  are constant. Then

$$\Delta\sigma = \sum_i \Delta\sigma_i = \sum_i q_i \mu_i \Delta N_i$$

and

$$\frac{\Delta\sigma}{\sigma} = \frac{\sum_i q_i \mu_i N_i (\Delta N_i / N_i)}{\sum_i q_i \mu_i N_i}$$

Because the sound wave acts uniformly on all the constituents of the medium,  $\frac{\Delta N_i}{N_i}$  equals  $\frac{\Delta \rho}{\rho}$ , where  $\rho$  is the density of the medium. Note that  $\frac{\Delta \rho}{\rho}$  is independent of the summation in the above equation. Thus,

$$g(\rho) = \left( \frac{\Delta \sigma}{\sigma} \right)_T = \frac{\Delta \rho}{\rho} \frac{\sum_i q_i \mu_i N_i}{\sum_i q_i \mu_i N_i} = \frac{\Delta \rho}{\rho} .$$

The total change in conductivity is given by

$$g = \frac{\Delta \sigma}{\sigma} = \left( \frac{\Delta \sigma}{\sigma} \right)_\rho + \left( \frac{\Delta \sigma}{\sigma} \right)_T = g(T) + g(\rho).$$

The conductivity perturbation was calculated for four different concentrations of salt water at 25° C. These results are presented in Table I.

TABLE I

PREDICTED FRACTIONAL CHANGE OF CONDUCTIVITY

<u>Molal Concentration</u>	<u>g(T)</u>	<u>g(ρ)</u>	<u>g</u>
0.3	4.04	4.31	8.35
0.6	4.11	4.16	8.27
1.5	3.84	3.76	7.60
3.0	3.94	3.20	7.14

Note: Data are for aqueous sodium chloride solutions at 25° C. The unit of g is 10<sup>-11</sup> per dyne/cm<sup>2</sup>.

### 3. Dielectric Constant

Again from the data of Saxton and Lane, empirical expressions of the form

$$\epsilon_r = A' - B'T \quad (7)$$

can be derived for the static dielectric constant as a function of temperature over the range of 0° to 40° C. In this expression,  $\epsilon_r$  is the dielectric constant, T is the temperature in degrees centigrade, and A' and B' are constants depending on the concentration. Values of these constants for the four sodium chloride solutions used are listed below.

<u>Molality</u>	<u>A'</u>	<u>B'</u>
0.3	81.2	0.327
0.6	75	0.285
1.5	62	0.245
3.0	45.5	0.207

From the definition of f and Equation 7, it follows that

$$f(T) = \left( \frac{\Delta\epsilon_r}{\epsilon_r} \right)_\rho = \frac{-B' \Delta T}{A' - B'T}$$

Values of f(T) for the four solutions at 25° C appear in Table II.

Theoretical predictions of the fractional change in the dielectric constant of salt water produced by local variations in density caused by the sound wave are highly questionable because no adequate theory of strongly associated polar liquids such as water exists. Nevertheless, a prediction of the perturbation of the dielectric constant is included below according to the theory of Onsager.<sup>11</sup>

Onsager gives the following implicit expression for the dielectric constant

<sup>11</sup>L. Onsager, "Electric Moments of Molecules in Liquids," Journal of the American Chemical Society 58, 1486 (1936).

of a polar liquid:

$$\frac{(\epsilon_r - n^2)(2\epsilon_r + n^2)}{\epsilon_r(n^2 + 2)^2} = \frac{4\pi\mu_o^2 N}{9kT} ; \quad (8)$$

where  $\epsilon_r$  is the static dielectric constant,

$n$  is the optical index of refraction,

$\mu_o$  is the dipole moment in vacuo,

$N$  is the number of molecules per cubic centimeter,

$k$  is Boltzmann's constant,

and  $T$  is the Kelvin temperature.

For the present purpose, this may be written in the simpler form:

$$\frac{(\epsilon_r - n^2)(2\epsilon_r + n^2)}{\epsilon_r} = CN , \quad (9)$$

where

$$C = \frac{4\pi\mu_o^2(n^2 + 2)^2}{9kT} .$$

Taking the variation of both sides of Equation 9 gives

$$\frac{2\epsilon_r^2 + n^4}{\epsilon_r^2} \Delta\epsilon_r = C \Delta N = CN \frac{\Delta N}{N} .$$

Substituting for  $CN$  from Equation 9 and simplifying gives

$$\frac{\Delta\epsilon_r}{\epsilon_r} = \frac{(\epsilon_r - n^2)(2\epsilon_r + n^2)}{2\epsilon_r^2 + n^4} \frac{\Delta N}{N} .$$

As before,  $\frac{\Delta N}{N} = \frac{\Delta \rho}{\rho}$ , where  $\rho$  is the density of the medium. Thus,

$$f(\rho) = \left( \frac{\Delta \epsilon_r}{\epsilon_r} \right)_{\rho} = \frac{(\epsilon_r - n^2)(2\epsilon_r + n^2)}{2\epsilon_r^2 + n^4} \frac{\Delta \rho}{\rho} \quad (10)$$

From this expression, it is seen that for the high dielectric constants typical of salt water solutions  $f(\rho)$  is approximately equal to the fractional change in density. This result also follows from a similar treatment of Kirkwood's theory.<sup>12</sup>

Values of  $f(\rho)$  for four different concentrations of aqueous sodium chloride solution calculated from Equation 10 are presented in Table II. It should be pointed out that Equations 8 and 10 were derived to describe the behavior of pure polar liquids, not electrolytic solutions. The only way in which the presence of dissolved salt is taken into account is in adjustment of the value of  $\epsilon_r$ . The dielectric constant of the solution was used in making the numerical computations.

The total fractional change of the dielectric constant is represented by

$$f = \frac{\Delta \epsilon_r}{\epsilon_r} = f(T) + f(\rho) = \left( \frac{\Delta \epsilon_r}{\epsilon_r} \right)_{T} + \left( \frac{\Delta \epsilon_r}{\epsilon_r} \right)_{\rho}$$

Values of  $f$  also appear in Table II.

<sup>12</sup>J. G. Kirkwood, "The Dielectric Polarization of Polar Liquids," Journal of Chemical Physics 7, 911 (1939).

TABLE II

PREDICTED FRACTIONAL CHANGE OF DIELECTRIC CONSTANT

<u>Molal Concentration</u>	<u>f(T)</u>	<u>f(ρ)</u>	<u>f</u>
0.3	-0.98	4.25	3.27
0.6	-0.93	4.10	3.17
1.5	-0.96	3.69	2.73
3.0	-1.12	3.12	2.00

Note: Data are for aqueous sodium chloride solutions at 25° C. The unit of f is 10<sup>-11</sup> per dyne/cm<sup>2</sup>.

#### D. Instrumentation

The measurement equipment used is illustrated schematically in Figure 3. The equipment is arranged to allow an accurate comparison between the modulation produced by the water perturbation and the calibrated modulator of the signal generator.

The output of the signal generator enters the coaxial hybrid ring by arm No. 1 and is equally divided between arms 2 and 4. Arm 4 is terminated by a matched load, and arm 2 is connected to the coaxial test cell. The power incident on the test cell is reflected at the water surface, and is divided again in the hybrid ring between arms 1 and 3. The latter arm contains a matched amplitude detector, the output of which feeds a tuned amplifier and indicator. The important characteristics of each of these components and the measurement procedure are described in the Appendix.

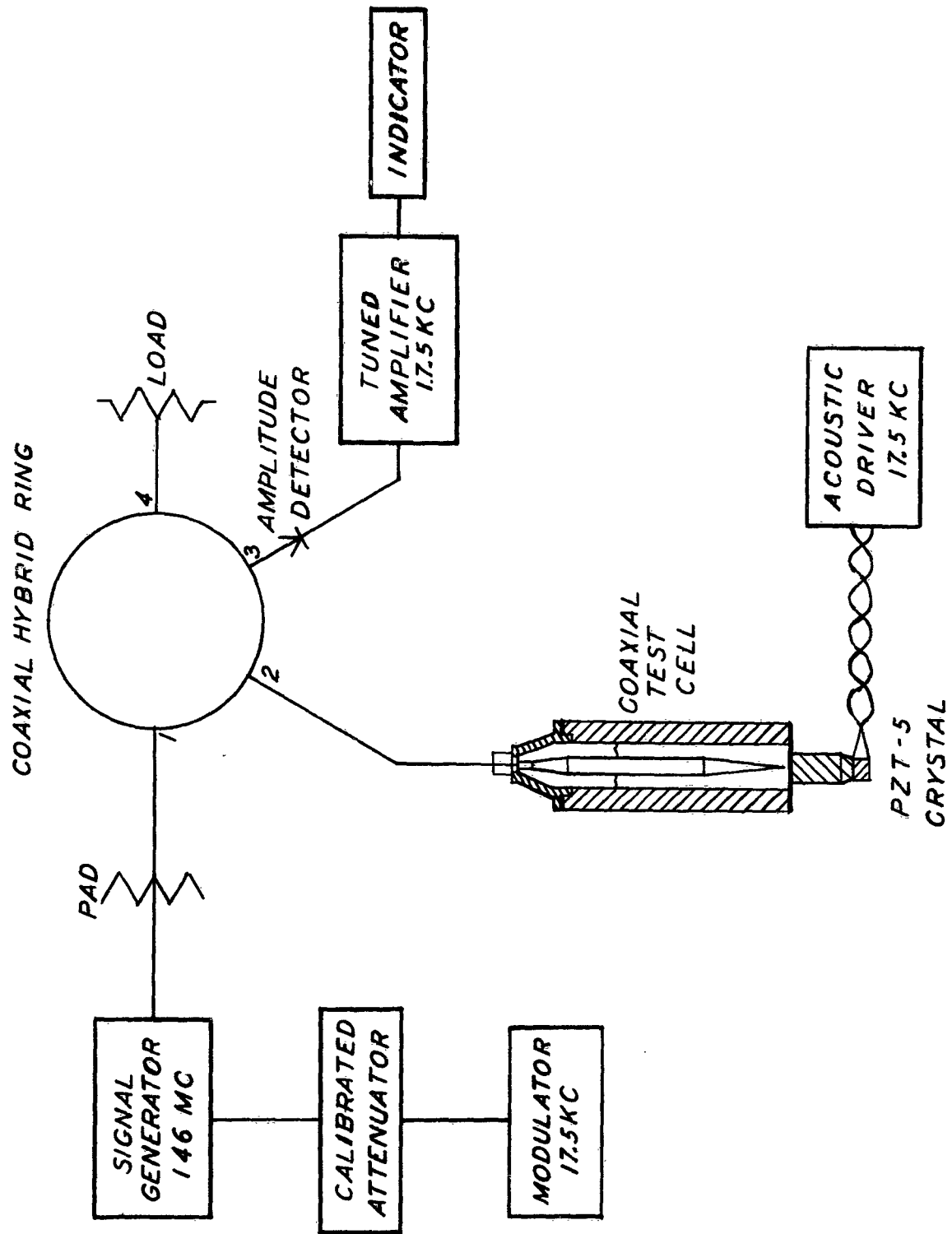


Figure 3. Equipment for Measurement of Acoustic-Radio Interaction.

E. Results of Measurements

Data have been obtained at a radio frequency of 146 mc for five salt solutions: aqueous sodium chloride solutions of concentration 0.3, 0.6, 1.5, and 3 molal and an artificial sea water mixture prepared from the analysis of Subow. For each of these solutions, the observed amplitude modulation index per unit pressure is plotted against acoustic frequency in Figure 4. On each graph is drawn a curve of modulation per unit pressure calculated from Equation 4 for the parameter  $f = 0$  and for a value of  $g$  chosen in each case to best fit the data. The Subow mixture is assumed to have the same electrical parameters as the 0.6-molal sodium chloride solution for purposes of evaluating Equation 4 and establishing the value of  $g$ .

In Table III are compared the experimentally determined values of  $g$  for each of the solutions and the values of  $g$  predicted in Section C. The agreement is remarkable in view of the uncertainty in the measurements, and it is probably accidental.

The result for the 0.6-molal solution is in agreement with the measurements at low frequencies by Fox, Herzfeld, and Rock on the bulk conductivity.

The error brackets shown in Figure 4 represent the rms deviations from the mean of the observations. The data were assumed to be log normal. Four to six measurements were made at each point. In addition to this spread, there are absolute errors due to the standard hydrophone and the voltmeter used to establish the pressure, and there is a relative error in the calibrated attenuator. These calibration errors are estimated not to exceed a total of 2.5 db. In applying this calibration error, it should be remembered that  $g$ ,  $m$ , and  $p_a$  are all amplitudes. The rather large spread in the observations is due to instabilities

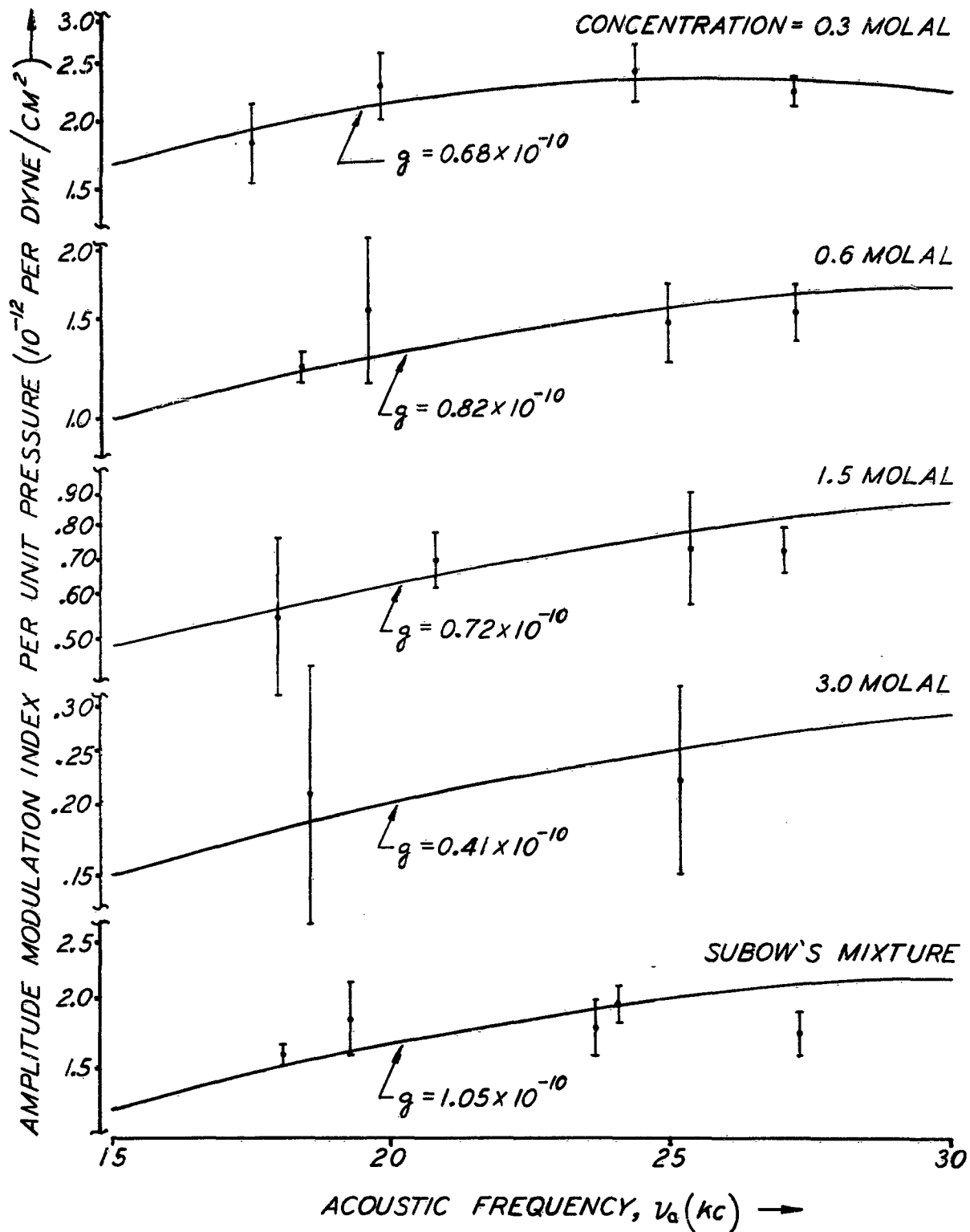


Figure 4. Experimentally Determined Amplitude Modulation Index per Unit Pressure for Aqueous Sodium Chloride Solutions at 27° C.

TABLE III

COMPARISON OF EXPERIMENTALLY DETERMINED AND PREDICTED VALUES OF  $g$

<u>Molal Concentration</u>	$g = \frac{d\sigma}{\sigma}$	
	<u>Measured</u>	<u>Predicted</u>
0.3	0.68	0.84
0.6	0.82	0.83
1.5	0.72	0.76
3.0	0.41	0.71
Subow's mixture	1.05	--

Note: Data are for sodium chloride solutions at 27° C;  $g = \frac{d\sigma}{\sigma}$  is in units of  $10^{-10}$  per dyne/cm<sup>2</sup>.

in the various instruments. Although reasonable care was exercised in the design and use of the instruments and in the use of stabilized power supplies for both filaments and plates, the large number of independent instruments and very narrow bandwidths necessary limited the accuracy of a single observation.

It was argued in Section C that an increase in pressure in the salt solution produced an increase in the conductivity of the solution. Further, one expects that the wave reflected from the surface should increase in amplitude if the conductivity of the surface increases. The analysis of Schmitt and the calculations in this report based on his work agree with this. Thus, one expects that an increase in pressure (compression) near the surface of the water should result in positive deflection of the amplitude of the carrier reflected from the water surface. After a very careful account was taken of the phase shift of each instrument, this phase relationship was found to

exist. The polarity of the acoustic probe crystal was found in a direct manner by noting the charge polarity at the probe terminals as the probe was compressed statically in a small tank.

III. SUMMARY

The following summarizes the results of this investigation:

1. The fractional change in the conductivity of aqueous sodium chloride solutions has been measured by observing the modulation of an electromagnetic wave reflected from the water surface; it was found to be of the order of  $0.7 \times 10^{-10}$  per dyne/cm<sup>2</sup> pressure change.

2. The measured value of conductivity change is consistent with predictions of static changes based on simple assumptions and empirical data of the dependence of conductivity on temperature and density.

3. The measurements are consistent with those of Fox, Herzfeld, and Rock on the bulk conductivity of salt water at low radio frequencies.

4. Instrumentation has been assembled that is capable of measuring modulation levels lower than 160 db below 100 per cent for one cycle per second of bandwidth.

5. The data taken at a radio frequency of 146 mc and acoustic frequencies of 15 to 30 kc contain no information on the magnitude of dielectric constant perturbation relative to conductivity perturbation. Measurements at a radio frequency near 1000 mc will be required to determine the magnitude of the dielectric constant change with pressure.

IV. ACKNOWLEDGMENTS

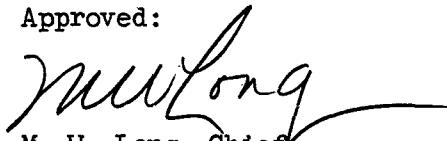
The helpful advice of Dr. Maurice W. Long and the support of Dr. Arnold Shostak are gratefully acknowledged.

Respectfully submitted:



W. K. Rivers, Jr.  
Project Director

Approved:



M. W. Long, Chief  
Electronics Division



J. E. Boyd, Director  
Engineering Experiment Station

V. APPENDIX

The unusual features and characteristics of the instruments used to make the measurements and the procedure followed are discussed in the following sections.

A. Radio-Frequency Equipment

The coaxial hybrid ring is constructed of RG-59/U cable with arms of RG-58-A/U cable. These cables have impedances of 73 and 50 ohms, respectively. The propagation factor for the RG-59/U was found to be 0.650; therefore, the circumference of the ring was made 200 cm for a design frequency of 146 mc. With matched loads on arms 2 and 4, the voltage standing wave ratio looking into arms 1 and 3 is less than 1.05 over a 2 per cent band. The isolation between arms 1 and 3 is greater than 45 db at the design frequency and is not less than 30 db over the 2 per cent band. Joints between the arms and the ring were made without the use of connectors by careful fitting of the dielectrics at the joint and with close conformity of the outer conductors to the joint.

The signal generator consists of a crystal-controlled oscillator followed by two frequency multipliers and a Class C amplifier stage. The output frequency is 146 mc, and the output power is about 10 watts into a 50-ohm load. The principal requirement of this signal source--besides the obvious ones of adequate power output and stability, which are not unusual--is that it have a very low level of noise modulation at the frequencies used for the acoustic waves. The noise level of this signal source is not known, and only an upper limit for the noise can be given. This is true because the detector described below saturates at a power level of approximately 2 mw, so that modulation

having an intensity lower than about 160 db below 100 per cent modulation per cycle per second of bandwidth could not be observed. The signal source used was compared with several others, some of which produced the same minimum detectable modulation index in conjunction with the detector described below; other signal sources had obviously higher noise levels, but none allowed lower minimum detectable modulation sidebands. It is concluded that the spectral density of noise modulation of the signal source used is lower than 163 db below 100 per cent modulation per cycle per second of bandwidth.

The noise characteristics of the signal source are probably determined by its output amplifier. Some of its parameters are displayed in Table IV. No attempt was made to optimize the noise performance of this stage, because the best detector available was only capable of setting an upper limit on the noise output of the amplifier.

TABLE IV

OPERATING PARAMETERS OF RADIO FREQUENCY GENERATOR OUTPUT AMPLIFIER

Tube type	2E26
Plate voltage	250 volts
Plate current	40 ma
Screen voltage	125 volts
Grid bias	28 volts
DC grid current	1.3 ma

The detector consists of a thermionic diode preceded by a radio frequency matching network. Its schematic is shown in Figure 5. The two halves of a 6AL5 diode are paralleled, and their shunt capacity is resonated at the radio

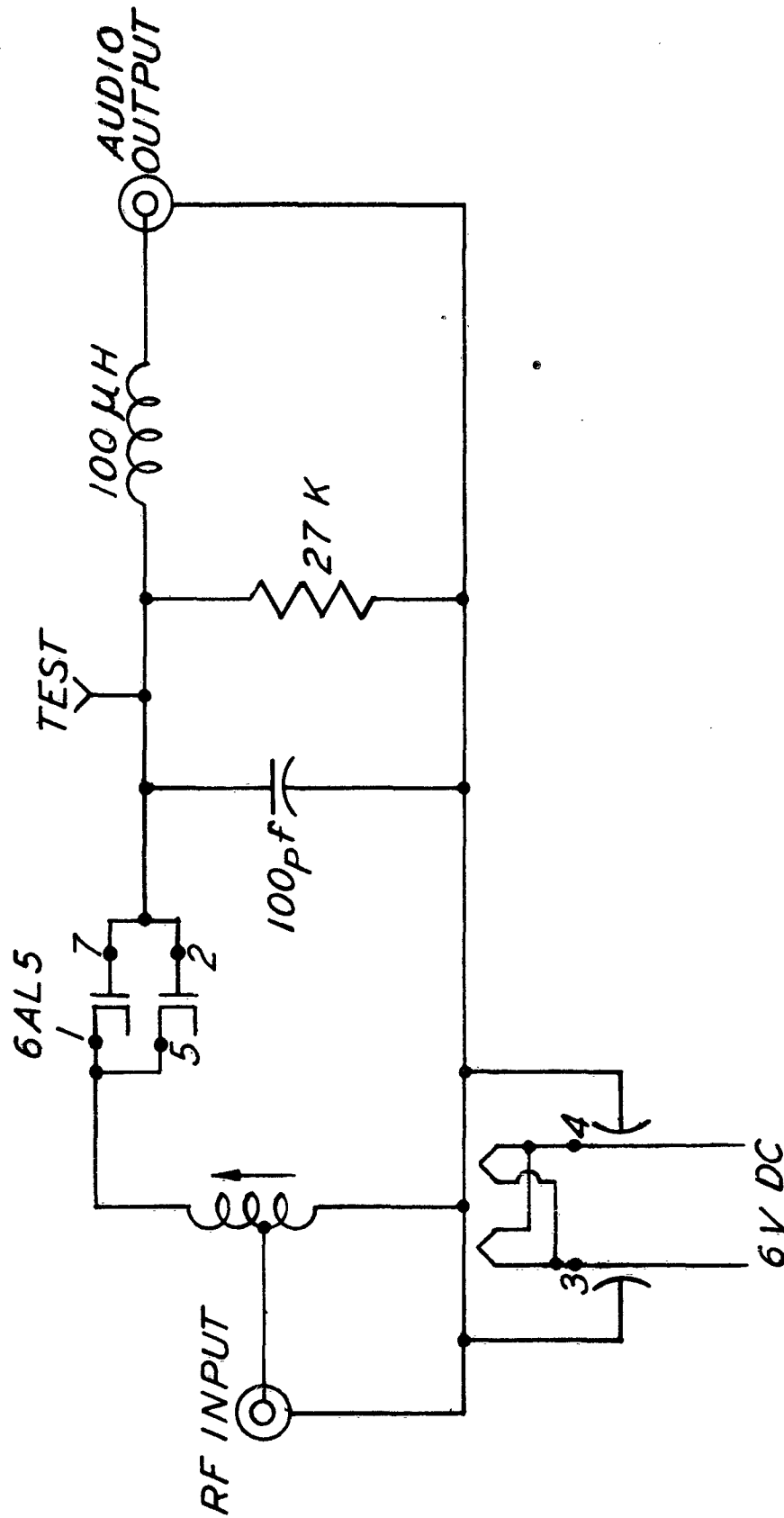


Figure 5. Amplitude Detector.

frequency by the adjustable input coil. The position of the tap on this coil is adjusted to present a 50-ohm input impedance.

The minimum detectable signal of an ideal detector of this type will be found by comparing signal and noise powers at the output of the detector rather than at the input. Consider, as in Figure 6, a carrier at frequency  $\nu$  with symmetrically located sidebands at frequencies  $\nu \pm \nu_a$ . An ideal generator at temperature  $T_0$  will have a noise power output of  $kT_0\Delta\nu$  in each of two bandwidths  $\Delta\nu$  about the sideband frequencies. Since the noise in these two sidebands can be considered to be uncorrelated in phase, these noise sidebands will mix with the carrier to produce a noise power in the detector output proportional to  $2kT_0\Delta\nu G$  where  $G$  is the conversion gain of the detector. However, the signal sidebands are correlated in phase and produce a power output from the detector of  $4P'G$ , where  $P'$  is the power of each signal sideband. In order to relate the total sideband power to the modulation index, consider the definition of  $m$ :

$$E = E_0 (1 + m \cos \omega_a t) \quad .$$

Find the total average power by squaring this and integrating over one cycle.

$$\begin{aligned} P = P_0 + 2P' &= \frac{1}{2\pi} \int_0^{2\pi} P_0 (1 + 2m \cos \omega_a t + m^2 \cos^2 \omega_a t) d\omega_a t \\ &= P_0 (1 + m^2/2) \quad . \end{aligned}$$

Thus  $P' = P_0 m^2/4 \quad .$

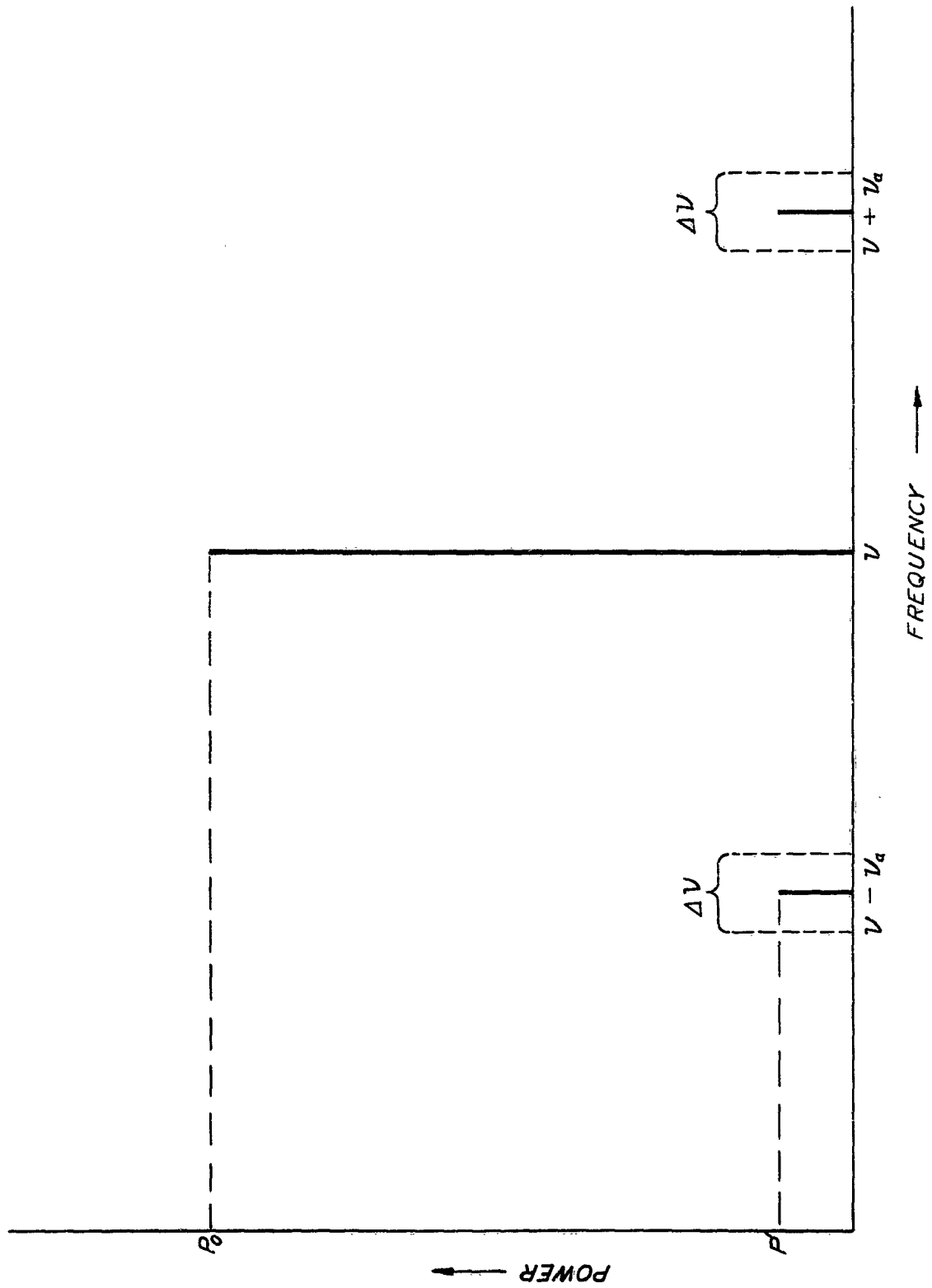


Figure 6. Spectrum of Amplitude Modulated Carrier.

The signal and noise powers both before and after the detector are compared in Table V.

TABLE V  
COMPARISON OF SIGNAL AND NOISE POWERS BEFORE AND AFTER DETECTION

	<u>Before Detection</u>	<u>After Detection</u>
Signal power	$(m^2/2)P_o$	$m^2P_oG$
Noise power	$2kT_o \Delta\nu$	$2kT_o \Delta\nu G$

Although the criteria applied to determine minimum detectable signals of systems are arbitrary, it is believed that the experimentalist will require that the minimum detectable signal power equal the noise power on the output of the detector. Using this criterion, one finds

$$m_{\min} = \left[ \frac{2kT_o \Delta\nu}{P_o} \right]^{1/2}$$

The operation of the diode as a detector in the system described above is similar to that of a mixer in a superheterodyne; the essential difference is the presence of two signal sidebands in the former case. It is reasonable to expect that data on the performance of devices as mixers would also be applicable to the present detection problem. It has been found<sup>13</sup> that a

<sup>13</sup>M. W. Long, "Detectors for Microwave Spectrometers," Review of Scientific Instruments 31, 1286 (1960).

reasonable extension can be made of the parameters quoted for microwave mixer crystal diodes from the test intermediate frequency of 30 mc to much lower intermediate frequencies. According to reference 13, the noise ratio of a crystal diode for high power, where the crystal characteristic is linear, can be represented by

$$N_c = 1 + \frac{\gamma_c P_o}{v_a} \quad (11)$$

The first term of this noise ratio represents the Johnson noise of the diode, and the second term is a frequency dependent excess noise due to the diode current. Some good crystal mixers are reported to have noise ratios of 1.3 at an intermediate frequency of 30 mc and for a 1 mw power level. Use of these figures in Equation 11 predicts a noise ratio of 450 for an intermediate frequency of 20 kc and the same power level.

For the thermionic diode, an expression similar to Equation 11 can be written

$$N_d = 2.2 + \frac{\gamma_d}{v_a} \quad (12)$$

where the first term represents the space-charge-limited shot noise of a diode,<sup>14</sup> and the second term represents the frequency dependent flicker noise typical of vacuum tubes. Because there appears to be available no data on the performance of thermionic diodes as mixers, in order to estimate the noise ratio it will be necessary to assume that the diode possesses a flicker noise

---

<sup>14</sup>A. Van der Ziel, Noise, Prentice-Hall, Inc., Englewood Cliffs, New Jersey (1956), Section 5-1d.

resistance typical of a medium quality vacuum tube. For a flicker noise resistance  $R_{nf}$  of 100,000 ohms at 100 cps, the noise ratio is

$$N_d = 2.2 + R_{nf} g_m = 602 \quad ,$$

where a  $g_m$  of  $6 \times 10^{-3}$  mho is used for the diode conductance of the halves of a 6AL5 in parallel. At a frequency of 20 kc, the noise ratio might be expected to be

$$N_d = 2.2 + \frac{6 \times 10^4}{2 \times 10^4} = 5.2 \quad .$$

The predicted diode noise-ratio is seen to be about 20 db lower than that of the crystal diode at this modulation frequency.

In Figure 7 is plotted the minimum detectable modulation index as a function of the incident power for the thermionic diode and for radio and audio modulation frequencies of 146 mc and 17 kc, respectively. On the same graph, the calculated performance of a good crystal diode mixer is indicated for the same frequencies and for an assumed conversion gain of 0.3 with its plateau starting at 1 mw. The performance of the 6AL5 detector is seen to be consistent with the predicted noise ratio and a conversion gain of 0.35.

#### B. Acoustic Equipment

The acoustic pressure standard used in this experiment is a standard hydrophone type BM101A supplied by the Underwater Sound Reference Laboratory, Orlando, Florida. This hydrophone was used to calibrate small acoustic probes which were used to measure directly the pressure in the test cell.

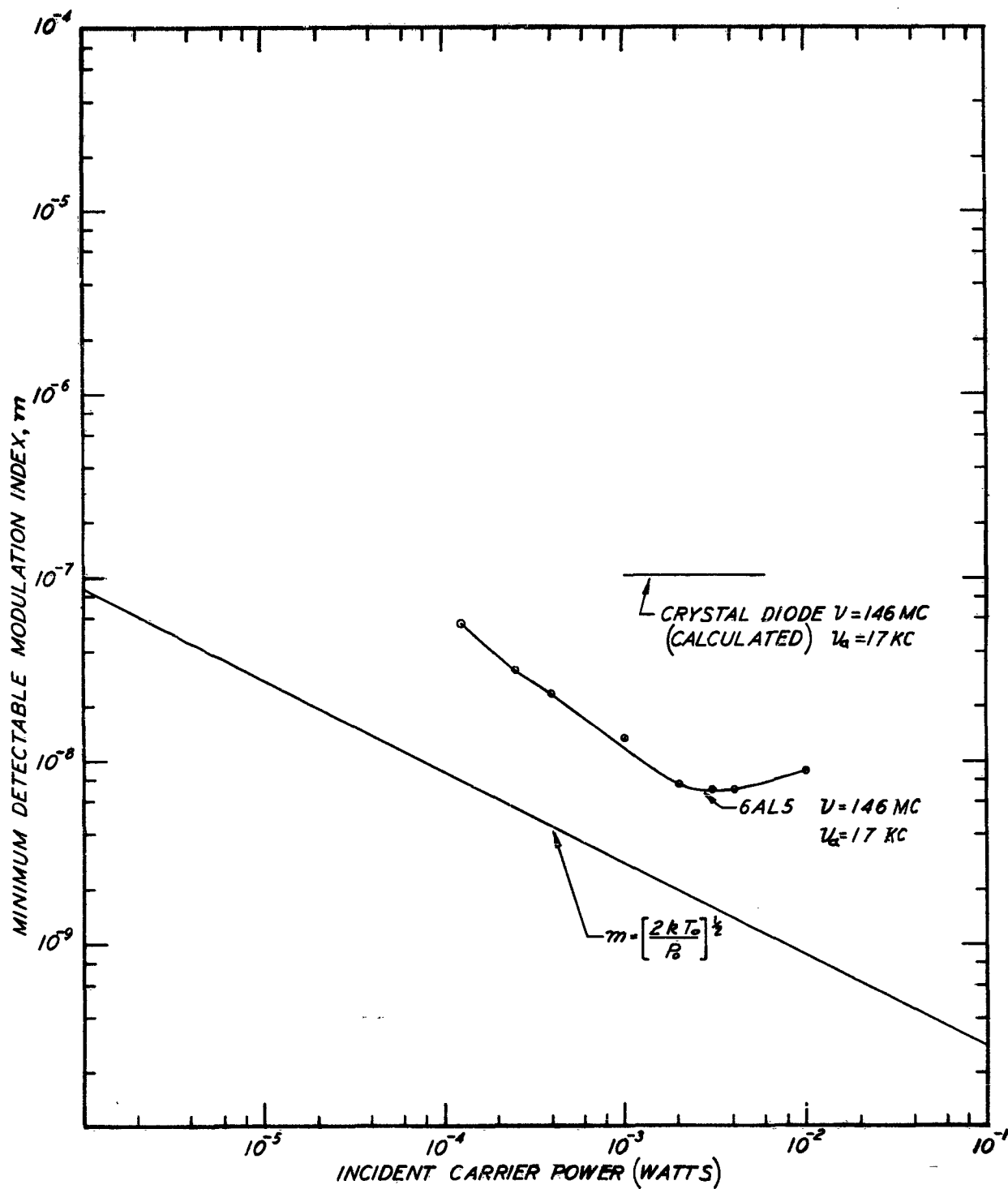


Figure 7. Minimum Detectable Modulation Index of Amplitude Detectors for a Bandwidth of One Cycle per Second.

Comparison of the sensitivities of the hydrophone and the probes was made in a tank 4 feet in diameter and 18 inches deep. The acoustic signal was a 25-kc carrier pulse of 0.2 millisecond duration generated by a transducer resting on the tank bottom. The hydrophone and probe were positioned in a uniform region of the field above the transducer and about 6 inches below the water surface. The outputs of the hydrophone and probe were viewed alternately on a Tektronix type 535 oscilloscope with a type 53C dual trace preamplifier. The probe output was amplified with a Tektronix type 121 wide-band preamplifier to compensate for the reduced sensitivity of the small probe compared with that of the standard hydrophone. The pulse outputs from the two hydrophones differed at no point within the pulse more than 2 per cent of the maximum voltage on the common oscilloscope display.

In Table VI below is shown a summary of probe calibration data.

TABLE VI  
SUMMARY OF PROBE CALIBRATION DATA

<u>Probe No.</u>	<u>Type</u>	<u>Mean Sensitivity (db)</u>	<u>RMS Deviation (db)</u>	<u>No. of Calibrations</u>
5	A	-29.8	0.95	7
6	A	-24.9	1.48	9
7	A	-27.2	1.20	7
7a	A	-26.6	0.43	11
8	A	-25.2	0.36	17
9	B	-24.3	0.44	7

Note: The mean sensitivity is given with respect to the EML01A hydrophone which has an output of -105 db with respect to one volt per microbar at 25 kc.

The reduced deviation of the calibrations in probes 7a, 8, and 9 is due to increased care in the handling of the probes; in particular allowing the probes to hang in water for long periods when not in use contributed heavily to the large deviations experienced with probes 5, 6, and 7.

The construction of the probes is illustrated in Figure 8. Probes of both types used tubes of PZT-5<sup>15</sup> ceramic transducer material plated on the inner and outer surfaces. Contacts were made between the plating and the No. 38 lead wires with silver paint. The probe handles were 0.086-inch OD, 50-ohm solid coaxial line. In the Type A probes, the crystal was suspended by the lead wires and the flexible Pliobond coating. Isolation between the crystal and the handle of this type was better than 30 db. The crystals of the Type B probes were mounted in a semirigid manner by a layer of Pliobond on the inner conductor of the coaxial handle. Handle isolation for this type was poor. The isolation measurements were made by comparing the crystal response when located at a pressure maximum of a standing wave near the water surface to the maximum response when the crystal was out of the water and the handle was in the sound field.

The construction of the coaxial test cell and its driver is illustrated in Figure 9. The hard-wall acoustic boundary conditions necessary to allow propagation of a plane wave in the water are created by the thick-walled stainless steel tube. The inside diameter of this tube was chosen to be below cut-off for modes of higher order than the plane wave in the water for frequencies below 30 kc. The water column is driven by the segmented resonant brass bar at the end of the tube. This bar is excited by a one-inch-diameter PZT-5

---

<sup>15</sup>Trademark of Clevite Electronic Components, a Division of Clevite Corporation, Cleveland, Ohio

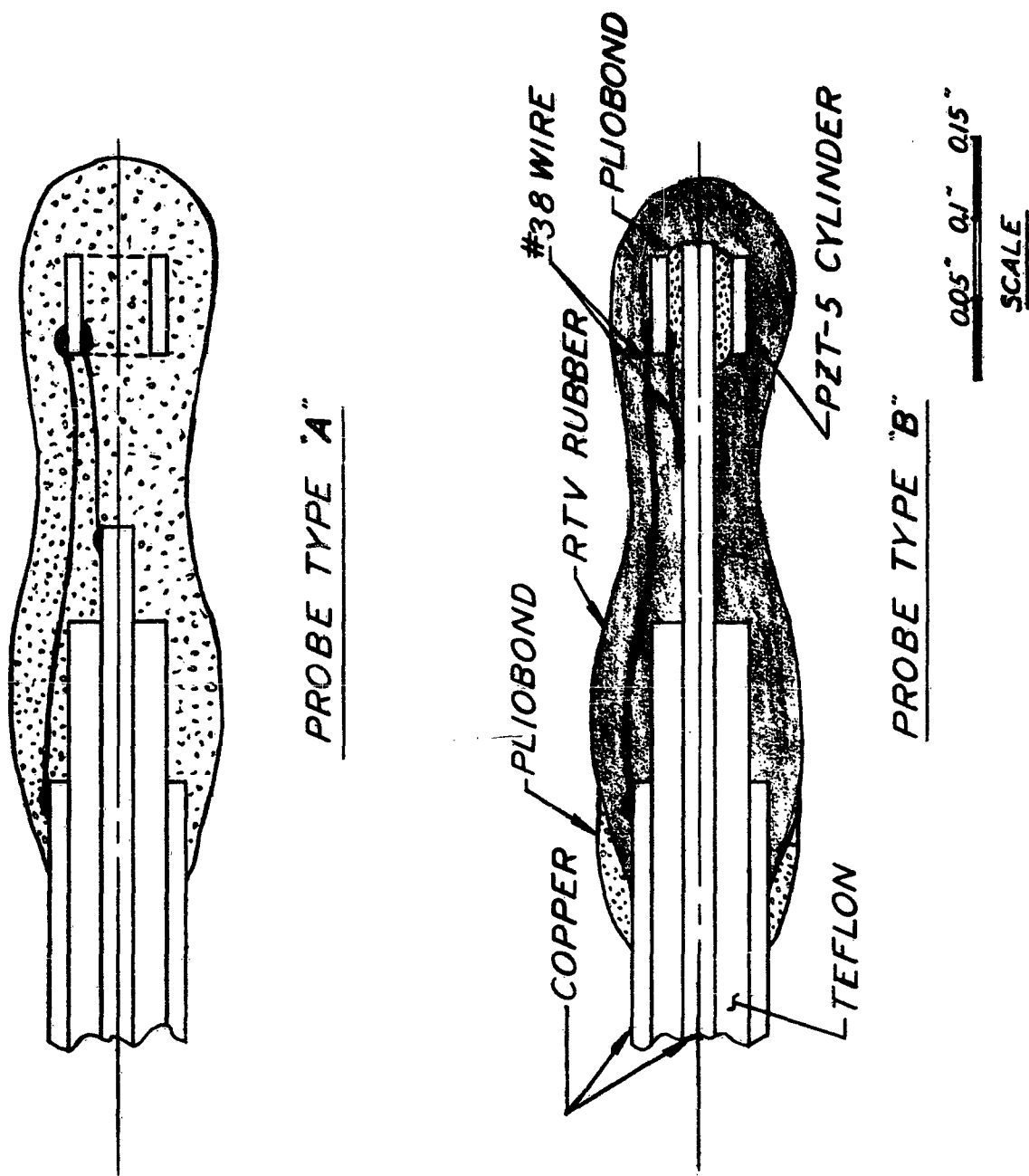


Figure 8. Acoustic Probe Construction.

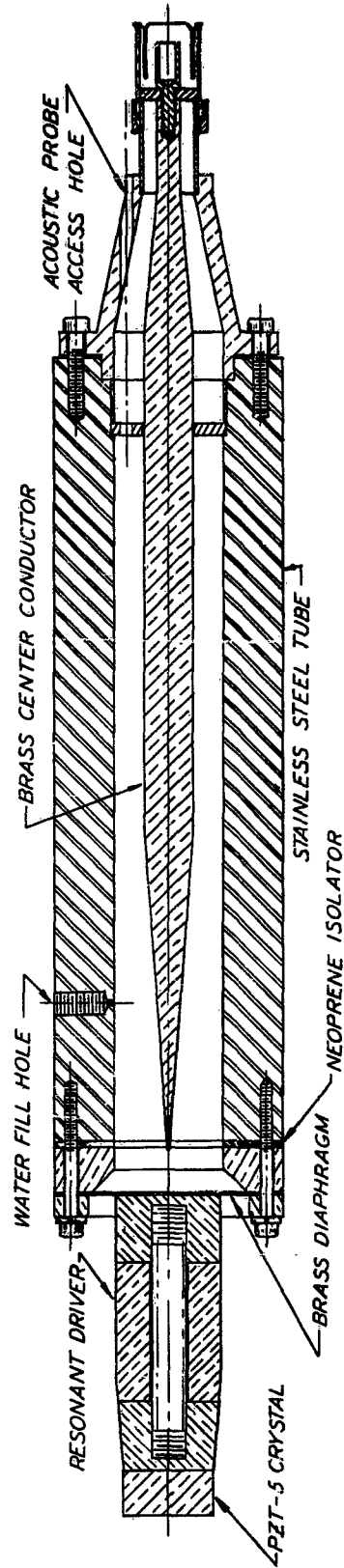


Figure 9. Coaxial Test Cell.

ceramic transducer element. Different bar lengths were used for the various acoustic frequencies.

Two difficulties which required special attention were encountered in the use of this test cell. One was caused by resonant vibrations of the stainless steel tube which produce a variation of the standing wave pattern along the length of the water column.<sup>16</sup> Since this effect was obvious only at certain frequencies, it was easy to avoid. For frequencies away from tube resonances and for correctly tuned water column heights, peak pressures of 0.2 atmosphere and pressure standing wave ratios exceeding 100 were obtained. The other difficulty was associated with the presence of air bubbles in the tube; this would not allow sound propagation in the water since the necessary hard-wall boundary condition could not be realized. The presence of air bubbles was troublesome for several hours after filling the tube with salt solution. During this period, the sound intensity in the water was distributed exponentially, decreasing upward from the transducer. This condition was relieved by raising the temperature of the salt solution near that of boiling to drive out some of the absorbed gases prior to filling the test cell.

The length of the uniform portion of the cell was sufficient to allow measurements on solutions having conductivities at least as great as that of 0.3-molal sodium chloride solution at two water levels a half-wavelength apart, but the length was too short to accommodate either low-loss liquids or pure water.

---

<sup>16</sup>E. Meyer, "Sound Absorption and Sound Absorbers in Water," Bureau of Ships, NavShips 900,164, ASTIA AD 140 720.

C. Measurement Procedure

The measurement of the acoustic modulation of conductivity consisted of the following distinct steps:

1. Acoustic probe calibration.
2. Measurement of  $p_a$ , the peak pressure in the cell.
3. Calibration of the modulator for the r-f source.
4. Comparison of interaction with the calibrated modulation.

The procedure for Step 1, the acoustic probe calibration, was described in Section B.

In Step 2, the probe is positioned at the peak of the first pressure maximum below the surface of the water in the cell. Its output is then compared with the output of the precision attenuator which is fed with a signal of the acoustic frequency at a level of one volt. The output of the probe determined in this way is used with the probe sensitivity found in Step 1 to calculate  $p_a$ .

The calibrated modulator for the r-f source was driven by the same precision attenuator used in Step 2. During the experiment the modulation level corresponding to zero attenuation was determined by measuring the ratio of the peak-to-peak swing to the d-c value of the plate voltage of the final r-f amplifier. Previously, it had been established that (a) the modulation level produced was linear from this point down to the noise within the accuracy and resolution of the precision attenuator, which is of the order of 0.1 db per 10 db plus 0.25 db, and (b) the modulation level deduced by observing the amplifier plate voltage is the same as that measured by observing directly the radio frequency output on the plates of an oscilloscope.

The comparison in Step 4 of the conductivity modulation with that produced by the r-f source modulator was made on an indicator whose deflection was produced by the averaged rectified output of the tuned amplifier. Since the indication produced by the acoustic wave was matched at the same level by the modulator, no corrections for the linearity of the detector and indicator were required.

There is a possibility of error in the measurement due to vibration of parts of the cell. This vibration causes a modulation of the r-f wave as the dimensions of the coaxial line and therefore its characteristic impedance change. In an effort to minimize the effect of cell vibration, data were taken and averaged for two water levels differing by one-half an acoustic wavelength. When a half-wavelength of water is added to the height of the water column, the phase of the pressure at the first maximum below the water surface is reversed with respect to that of the driver, and hence the phase of the conductivity modulation is reversed. But the phase of the driver and the pressure wave in the lower part of the cell is unaffected by the addition of a half-wavelength of water to the height. The phase of the output of the tuned amplifier was observed to follow exactly that of the pressure at the first maximum while the vibration amplitude and phase of the vibration of the coaxial center conductor changed only slightly as the water level was changed by a half-wavelength. The spread of results averaged for different water levels was small, so that it appears that the effects of cell vibrations were small compared to the conductivity modulation.

DISTRIBUTION

	<u>No. of Copies</u>
Assistant Secretary of Defense for Research and Engineering Information Office Library Branch Washington 25, D. C.	2
Armed Services Technical Information Agency Arlington Hall Station Arlington 12, Virginia	5
Chief of Naval Research Electronics Branch (Code 427) Department of the Navy Washington 25, D. C.	5
Director, Naval Research Laboratory Technical Information Officer Washington 25, D. C. (Code 2000)	6
Director, Naval Research Laboratory (Code 5400) Washington 25, D. C.	2
Commanding Officer ONR Branch Office 86 East Randolph Street Chicago 1, Illinois	1
Commanding Officer ONR Branch Office 1030 East Green Street Pasadena 1, California	1
Commanding Officer Office of Naval Research Navy No. 100, Box 39, F.P.O. New York, New York	1
Office of Technical Services Technical Reports Section Department of Commerce Washington 25, D. C.	1
Commander Air Force Office of Scientific Research (SRY) Washington 25, D. C.	2

DISTRIBUTION (Continued)

	<u>No. of Copies</u>
Commander U. S. Naval Air Missile Test Center Pt. Mugu, California	1
Director U. S. Naval Observatory Washington 25, D. C.	1
Dr. D. Alpert, Technical Director Control Systems Laboratory University of Illinois Urbana, Illinois	1
Research Laboratory for Electronics Massachusetts Institute of Technology Cambridge 39, Massachusetts	1
Department of Physics Columbia University New York 27, New York	1
Dr. E. L. Ginzton Microwave Research Laboratory Stanford University Stanford, California	1
Dr. Samuel Silver Electronics Research Laboratory University of California Berkeley 4, California	1
Dr. Nathan Marcuvitz Polytechnic Institute of Brooklyn 55 Johnson Street Brooklyn 1, New York	1
Commanding Officer ONR Branch Office 346 Broadway New York 13, New York	1
National Security Agency Division of Physical Sciences Fort George G. Meade, Maryland	1

DISTRIBUTION (Continued)

	<u>No. of Copies</u>
Electronics Research Directorate Air Force Cambridge Research Center Laurence G. Hanscom Field Bedford, Massachusetts Attention: Library	1
Office of Ordnance Research Box CM, Duke Station Durham, North Carolina	1
Technical Information Officer Signal Corps Engineering Laboratory Fort Monmouth, New Jersey	2
Director National Science Foundation Washington 25, D. C.	1
Director, National Bureau of Standards Department of Commerce Washington 25, D. C.	1
Chief, Bureau of Ships Department of the Navy Washington 25, D. C.	1
Chief, Bureau of Weapons Department of the Navy Washington 25, D. C.	1
Commander Naval Air Development and Material Center Johnsville, Pennsylvania	1
Librarian U. S. Naval Electronics Laboratory San Diego 52, California	1
Commanding Officer and Director U. S. Naval Underwater Sound Laboratory Fort Trumbull, New London, Connecticut	1
Librarian U. S. Navy Post Graduate School Monterey, California	1

DISTRIBUTION (Continued)

No. of  
Copies

Commanding Officer  
ONR Branch Office  
495 Summer Street  
Boston 10, Massachusetts

1